Direct eigenmode analysis of plasmonic modes in metal nanoparticle chain with layered medium

Jian-Wen Dong*,† and Zi-Lan Deng†

State Key Laboratory of Optoelectronic Materials and Technologies, Sun Yat-Sen University, Guangzhou 510275, China
**Corresponding author: dongjwen@mail.sysu.edu.cn*

Received March 12, 2013; revised May 29, 2013; accepted May 29, 2013;
posted May 29, 2013 (Doc. ID 186915); published June 24, 2013

Using the dyadic Green function (GF) with a multilayer medium, we propose an eigendecomposition (ED) analysis of a plasmonic system composed of a one-dimensional periodic metal nanoparticle chain and planar layered structure. An effective eigenpolarizability involving the collective effects of both the chain and the layered structure is well defined to characterize the dispersion relation and the mode quality of the plasmonic modes. Applying this method, we demonstrate that the interplay between the surface plasmon polaritons (SPPs) at the metal–dielectric interface and the localized plasmon in the chain enables strong mode splitting. In particular, for the polarization perpendicular to layer surface, high-quality modes can be present inside the light cone even if the chain is open to the surrounding air. A slow-light band is also predicted to exist as long as the layered medium supports a SPP mode that can couple to the chain mode.

OCIS codes: (260.3910) Metal optics; (130.2790) Guided waves; (240.6680) Surface plasmons; (260.2030) Dispersion.
http://dx.doi.org/10.1364/OL.38.002244

Plasmons, which are electromagnetic excitations at metal-insulator interfaces, have been widely used to overcome the diffraction limit. Many nanoscale devices can be utilized based on surface plasmon polaritons (SPPs), such as biosensors, subwavelength waveguides, and near-field imaging devices. A chain of metal nanoparticles (MNPs) can support the propagating of light on the subwavelength scale by the localized plasmon resonance coupling of MNPs [1]. Dispersion relations of the freestanding MNP chain can be obtained by the dyadic Green function (GF) in the coupled dipole approximation [2–5]. However, for fabrication process, a substrate is compulsory. When the chain is close to the metallic surface, there are many intriguing behaviors due to plasmonic coupling [6–9]. By employing an external source acting on a finite system, source-dependent plasmonic phenomena can be observed, which are plausible and sophisticated. A dynamic eigenmode analysis is required in order to deeply understand the mechanisms.

In this Letter, we apply an eigendecomposition (ED) method to study a MNP chain in layered medium. Compared with former methods, the ED method does not need the tedious search for roots in a complex plane, and one can simultaneously obtain the dispersion relation and the mode quality. In particular, we investigate the plasmonic modes in the MNP chain near the metallic surface. The system exhibits significant mode splitting behavior due to the strong coupling between the chain mode and the SPP mode. A mode with slow group velocity is found inside the light cone even if the chain is open to the surrounding air.

Consider a chain of MNPs that are small enough to be represented by dipoles; it is placed in front of a general three-layer medium (Fig. 1). Each particle has a dynamic dipole polarizability related to the Mie's coefficients [2]. Then we obtain

$$\mathbf{p}_m = 4\pi\varepsilon_0\alpha(\omega)\begin{bmatrix}\mathbf{E}_m^{\text{ext}} + \omega^2\mu_0\sum \overleftrightarrow{\mathbf{G}}^{\text{sca}}(\mathbf{r}_m,\mathbf{r}_n)\mathbf{p}_n \\ +\omega^2\mu_0\sum_{n\neq m}\overleftrightarrow{\mathbf{G}}^{\text{free}}(\mathbf{r}_m,\mathbf{r}_n)\mathbf{p}_n\end{bmatrix}, \quad (1)$$

by using the coupled dipole equations, where $\mathbf{p}_m = (p_{mx}, p_{my}, p_{mz})^T$ is the induced dipole moment on the m th particle at $\mathbf{r}_m = (x_m, y_m, z_m)$. $\mathbf{E}_m^{\text{ext}}$ is the external source acting on the m th particle. $\overleftrightarrow{\mathbf{G}}^{\text{free}}$ is the GF of the freestanding chain itself. $\overleftrightarrow{\mathbf{G}}^{\text{sca}}$ represents the contribution by the scattering of the layered medium, with the form of

$$\overleftrightarrow{\mathbf{G}}^{\text{sca}}(\mathbf{r},\mathbf{r}') = \frac{i}{4\pi}\int_0^\infty \frac{dk_\parallel k_\parallel}{k_{2z}} \times \begin{bmatrix}(S_E^- e^{-ik_{1z}z}e^{ik_{2z}z'} + S_E^+ e^{ik_{1z}z}e^{ik_{2z}z'})\hat{\mathbf{E}}\hat{\mathbf{E}} \\ +S_H^- e^{-ik_{1z}z}e^{ik_{2z}z'}\hat{\mathbf{H}}(-k_{1z})\hat{\mathbf{H}}(-k_{2z}) \\ +S_H^+ e^{ik_{1z}z}e^{ik_{2z}z'}\hat{\mathbf{H}}(k_{1z})\hat{\mathbf{H}}(-k_{2z})\end{bmatrix}, \quad (2)$$

where $k_{iz}^2 + k_\parallel^2 = \varepsilon_i k_0^2$, $i = 1$, represents field layer and $i = 2$ represents source layer. $k_0 = \omega/c$ with c as the speed of light. $\mathbf{r} = (x, y, z)$ is the field position and $\mathbf{r}' = (x', y', z')$ is the source position. $\hat{\mathbf{E}}\hat{\mathbf{E}}$ and $\hat{\mathbf{H}}\hat{\mathbf{H}}$ can be found in [10]. $S_E^\pm$ and $S_H^\pm$ are complex amplitudes for transverse electric (TE) and transverse magnetic (TM) polarization, respectively. In our case, the chain is at $z = 0$ in layer 1, so $z = z' = 0$, $S_E^+ = R^{\text{TE}}$, $S_H^+ = R^{\text{TM}}$, $S_E^- = S_H^- = 0$, where R^{TE} and R^{TM} are the reflection coefficients of the slab [10].

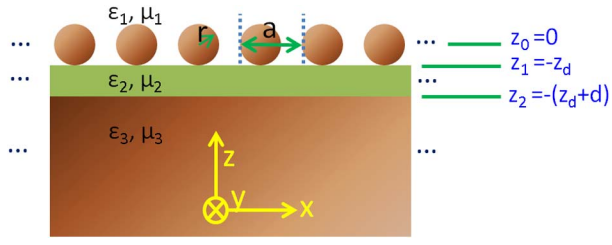

Fig. 1. Periodic MNP chain on a three-layered medium. The chain is in the (ε_1, μ_1) medium. The neighboring media are (ε_2, μ_2) and (ε_3, μ_3).

In fact, Eq. (1) can be written in a matrix form,

$$[\mathbf{M}]_{3N\times 3N}\mathbf{p} = [\mathbf{E}^{\text{ext}}], \tag{3}$$

and $[\mathbf{M}] = \alpha^{-1}[\mathbf{I}] - 4\pi k_0^2[\mathbf{G}^{\text{sca}}] - 4\pi k_0^2[\mathbf{G}^{\text{free}}]$ is a $3N \times 3N$ matrix, and $\mathbf{p}$ is a $3N$ column vector. Because of the translation symmetry of the studied system, we can assume $\mathbf{p}_m = \tilde{\mathbf{p}}\exp(ikma)$ and $\mathbf{E}_m^{\text{ext}} = \mathbf{E}_0\exp(ikma)$. Then Eq. (3) can be reduced to a 3×3 matrix equation by Bloch's theorem,

$$[\tilde{\mathbf{M}}(k,\omega)]_{3\times 3}\tilde{\mathbf{p}} = (\alpha^{-1}[\tilde{\mathbf{I}}] - [\tilde{\mathbf{G}}^{\Sigma,\text{sca}}] - [\tilde{\mathbf{G}}^{\Sigma,\text{free}}])\tilde{\mathbf{p}} = [\tilde{\mathbf{E}}_0], \tag{4}$$

where $\tilde{\mathbf{p}} = (p_x, p_y, p_z)^T$ and k is Bloch wave vector. The GFs in Eq. (4) have the forms of

$$\tilde{\mathbf{G}}^{\Sigma,\text{free}} = 4\pi k_0^2 \sum_{n=-\infty,n\neq 0}^{+\infty} \overleftrightarrow{\mathbf{G}}^{\text{free}}(na\hat{\mathbf{x}},\hat{\mathbf{0}})e^{-ikna} = \begin{pmatrix} G_l^{\Sigma,\text{free}} & 0 & 0 \\ 0 & G_t^{\Sigma,\text{free}} & 0 \\ 0 & 0 & G_t^{\Sigma,\text{free}} \end{pmatrix}, \tag{5}$$

$$\tilde{\mathbf{G}}^{\Sigma,\text{sca}} = 4\pi k_0^2 \sum_{n=-\infty}^{+\infty} \overleftrightarrow{\mathbf{G}}^{\text{sca}}(na\hat{\mathbf{x}},\hat{\mathbf{0}})e^{-ikna} = \begin{pmatrix} G_{xx}^{\Sigma,\text{sca}} & 0 & G_{xz}^{\Sigma,\text{sca}} \\ 0 & G_{yy}^{\Sigma,\text{sca}} & 0 \\ G_{zx}^{\Sigma,\text{sca}} & 0 & G_{zz}^{\Sigma,\text{sca}} \end{pmatrix}, \tag{6}$$

In Eq. (5), $G_l^{\Sigma,\text{free}}$ and $G_t^{\Sigma,\text{free}}$ correspond to the longitudinal and transverse mode of the freestanding chain itself, and $G_l^{\Sigma,\text{free}} = -2ik_0a\Sigma_2 + 2\Sigma_3$, $G_t^{\Sigma,\text{free}} = k_0^2a^2\Sigma_1 + ik_0a\Sigma_2 - \Sigma_3$, where $\Sigma_n = \text{Li}_n(\exp[i(k_0-k)a]) + \text{Li}_n(\exp[i(k_0+k)a])$ and Li_n is an n th polylogarithm function. Note that Eq. (6) is a block diagonal matrix. As a result, the mode can be decomposed to the pure-y and the mixed-xz polarization. The components in Eq. (6) have to be treated by numerical integration, and are related to Bessel functions $J_i(x)(i = 0, 1, 2)$ as follows:

$$G_{xx}^{\Sigma,\text{sca}} = \sum_{n=-\infty}^{\infty} ik_1^2e^{-ikna} \times \int_0^{\infty} \text{d}k_{\parallel}\frac{k_{\parallel}}{2k_{1z}}\begin{bmatrix} R^{\text{TE}}(J_0(k_{\parallel}na) + J_2(k_{\parallel}na)) + \\ R^{\text{TM}}(J_0(k_{\parallel}na) - J_2(k_{\parallel}na))\frac{k_{1z}^2}{k_1^2} \end{bmatrix}, \tag{7a}$$

$$G_{yy}^{\Sigma,\text{sca}} = \sum_{n=-\infty}^{\infty} ik_1^2e^{-ikna} \times \int_0^{\infty} \text{d}k_{\parallel}\frac{k_{\parallel}}{2k_{1z}}\begin{bmatrix} R^{\text{TE}}(J_0(k_{\parallel}na) - J_2(k_{\parallel}na)) + \\ R^{\text{TM}}(J_0(k_{\parallel}na) + J_2(k_{\parallel}na))\frac{k_{1z}^2}{k_1^2} \end{bmatrix}, \tag{7b}$$

$$G_{zz}^{\Sigma,\text{sca}} = \sum_{n=-\infty}^{\infty} ik_1^2e^{-ikna}\int_0^{\infty} \text{d}k_{\parallel}\frac{k_{\parallel}}{k_{1z}}\left[R^{\text{TM}}J_0(k_{\parallel}na)\frac{k_{\parallel}^2}{k_1^2}\right], \tag{7c}$$

$$G_{xz}^{\Sigma,\text{sca}} = G_{zx}^{\Sigma,\text{sca}} = \sum_{n=-\infty}^{\infty} k_1^2e^{-ikna}\int_0^{\infty} \text{d}k_{\parallel}\frac{k_{\parallel}}{k_{1z}}\left[R^{\text{TM}}J_1(k_{\parallel}na)\frac{k_{1z}k_{\parallel}}{k_1^2}\right]. \tag{7d}$$

Consider the eigenvalue problem, $|\tilde{\mathbf{M}}(k,\omega)|\tilde{\mathbf{p}} = \lambda\tilde{\mathbf{p}}$, where λ is the eigenvalue of the matrix; then we can define the effective eigenpolarizability $\alpha_{\text{eig}} = 1/\lambda$ to represent the response of the whole system, as it has the dimension of polarizability [2]. By carefully checking Eqs. (4)–(6), we have $\lambda = \alpha^{-1} - \kappa^{\text{free}} - \kappa^{\text{sca}}$. So the eigenpolarizability (α_{eig}) is contributed not only by the intrinsic polarizability of the particle (α^{-1}), but also by the scattering of freestanding particles (κ^{free}) and the scattering between particles and the layered medium (κ^{sca}). Hence we deal with not only the coupling of individual particles in the chain, but also the intercoupling between the chain and the multilayer. The eigenpolarizability is proportional to the extinction of the driving field, and the width of an extinction peak is proportional to the mode quality. The peak frequency of $\text{Im}(\alpha_{\text{eig}})$ at a given k can be used to identify the resonant frequency, and the peak linewidth can define the quality factor of the mode. For a plasmonic mode, the narrower the linewidth, the higher the quality factor.

The ED method can be applied to study the coupling between the localized modes of the chain and the SPP mode of metallic surface. One can tune the dielectric thickness so as to make the plasmonic coupling strong enough to observe. Two cases are studied to demonstrate the coupling mechanism. One is the air–ITO (indium-tin oxide) interface without a metallic layer for comparison, with the parameters $(\varepsilon_3, \mu_3) = (3.8, 1)$, and $d = 0$. Another is an air–ITO–silver layered medium, with the parameters of $(\varepsilon_2, \mu_2) = (3.8, 1)$, $(\varepsilon_3, \mu_3) = (\varepsilon_{\text{silver}}, 1)$, and $d = 5$ nm for strong coupling. In both cases, silver is described by the Drude model $\varepsilon_{\text{silver}}(\omega) = \varepsilon_\infty - \omega_p^2/\omega(\omega + i\gamma)$, with $\varepsilon_\infty = 3.7$, $\omega_p = 9.08$ eV, and $\gamma = 0.018$ eV. The particle radius is $r = 25$ nm, and the lattice constant of the chain is $a = 75$ nm. $z_d = 25$ nm; so the MNPs are just above the ITO layer. Note that the particle size and the period will shift the resonant frequency. The space between the MNP and the metallic surface will influence the coupling strength. The larger the spacing, the lower the coupling and the smaller the splitting interval.

Figures 2(a)–2(c) show the intensity plot of $\log[\text{Im}(\alpha_{\text{eig}})]$ of the chain on an ITO substrate with three different polarizations. Here "main-x" or "-z" is used to label the dominant direction of the dipole moments along the x or z direction, although the dominant directions may sometimes exchange places with each other near the zone boundary at high frequencies. As the studied system is open boundary and the dissipation loss in metal is considered, both radiation and dissipation losses can reduce and broaden the value of $\text{Im}(\alpha_{\text{eig}})$. It is interesting to see that the trajectories of the air cone and the glass cone clearly appear in the band structure, and three kinds of modes can be identified easily. Guided modes in which energy is mostly confined along the chain have a high quality factor and are well represented below the glass cone, with the narrowest linewidth. Modes between

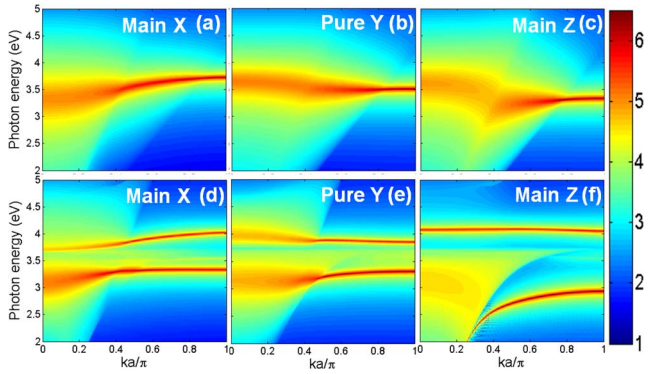

Fig. 2. Dispersion relation of a plasmonic chain on layered medium. (a)–(c) Case I: air–ITO with $d = 0$. (d)–(f) Case II: air–ITO–silver with $d = 5$ nm. $z_d = 25$ nm in both cases. Left, middle, and right columns correspond to the polarization of main-x, pure-y, and main-z, respectively. Red indicates resonant guided modes of the whole plasmonic system.

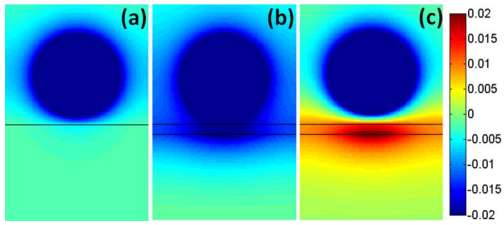

Fig. 3. Field distribution at $k = 0$ at the resonant frequency for pure-y polarization. (a) Air–ITO. (b), (c) Upper and lower mode in air–ITO–silver, showing the in-phase and antiphase properties between the particles and the substrate.

the air cones and the glass cones have a smaller quality factor as light radiates outside, showing that linewidth are broader from the glass cone to the air cone for each polarization. Modes above the air cone are not well defined owing to severe radiation losses.

For the three-layer medium with silver substrate, as there is a SPP mode at the interface of the ITO and the silver, the plasmonic coupling between the chain mode and the SPP mode will be significantly enhanced. Such hybrid modes are demonstrated in the dispersion diagram in Figs. 2(d)–2(f). The trajectories of the air cone in the main-x and the pure-y polarizations, as well as the trajectories of the ITO–silver dispersion curve in the main-z polarization, are quite consistent with the analytical formalism. For each polarization, one can obviously see the mode splitting behavior by comparison of the single-mode picture without the silver substrate plotted in Figs. 2(a)–2(c). The coupling between the chain mode and the SPP mode is illustrated by the field patterns in Fig. 3. For the air–ITO case, the field is localized in the chain. However, for the air–ITO–silver case, there is field enhancement in the ITO–silver interface. It shows the in-phase and antiphase properties between the particles and the substrate.

Another result of the antiphase properties is that the guided modes can be well defined even inside the air cone. For example, there is a slow-light band near 4.08 eV in the main-z polarization in Fig. 2(f). The mode quality of the plasmonic mode inside the air cone is as

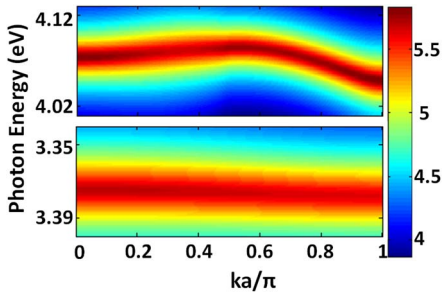

Fig. 4. Slow-light band in three-layer medium of (a) air–ITO–silver, same as Fig. 2(f) and of (b) silver–ITO–silver with the chain located in the ITO core layer.

good as that at the zone boundary, although the ambience of the chain is air. However, the value of $\mathrm{Im}(\alpha_{\mathrm{eig}})$ is not the same for all the Bloch vectors. Figure 4(a) shows the enlarged dispersion of Fig. 2(f) near 4.08 eV. The value of $\mathrm{Im}(\alpha_{\mathrm{eig}})$ decreases near $ka/\pi = 0.3$.

More simulations reveal that such a flat band is present as long as the layered medium supports a surface plasmon mode that couples to the localized chain mode. A representative example is the metal–dielectric–metal layered medium with the chain locating in the dielectric core. The corresponding dispersion is shown in Fig. 4(b). It is found that the group velocity is slightly negative.

In summary, we proposed an ED method to analyze the couplings between a MNP chain and a planar layered structure. The effective eigenpolarizability involving the collective plasmonic effects is obtained to simultaneously show the dispersion relation and the mode quality. In particular, we investigated hybrid plasmonic modes in the MNP chain near a metallic surface and found that there is a strong mode splitting behavior stemming from the strong coupling between the localized plasmon mode of the chain and the surface plasmon mode of the dielectric–metal interface. A slow-light band with high quality factor is found even inside the light cone of air due to its antiphase nature.

This work is supported by NSFC (11274396, 11074311), FRFCU (300003162498), GDNSF (S2012010010537), and OEMT.

†Both authors contributed equally to this work.

References

1. W. H. Weber and G. W. Ford, Phys. Rev. B **70**, 125429 (2004).
2. K. H. Fung and C. T. Chan, Opt. Lett. **32**, 973 (2007).
3. P. Holmström, L. Thylén, and A. Bratkovsky, Appl. Phys. Lett. **97**, 073110 (2010).
4. R. E. Noskov, P. A. Belov, and Y. S. Kivshar, Phys. Rev. Lett. **108**, 093901 (2012).
5. K. H. Fung, R. C. H. Tang, and C. T. Chan, Opt. Lett. **36**, 2206 (2011).
6. G. Leveque and R. Quidant, Opt. Express **16**, 22029 (2008).
7. D. Brunazzo, E. Descrovi, and O. J. F. Martin, Opt. Lett. **34**, 1405 (2009).
8. F. Zhou, Y. Liu, and Z.-Y. Li, Opt. Lett. **36**, 1969 (2011).
9. J. Cesario, R. Quidant, G. Badenes, and S. Enoch, Opt. Lett. **30**, 3404 (2005).
10. J. A. Kong, *Electromagnetic Wave Theory* (EMW, 2008).